Native Mass Spectrometry Imaging and In Situ Top-Down Identification of Intact Proteins Directly from Tissue

Hale, Oliver J.; Cooper, Helen J.

DOI:
10.1021/jasms.0c00226

ACS Partner Journal

Journal of the American Society for Mass Spectrometry

pubs.acs.org/jasms

Research Article

Native Mass Spectrometry Imaging and *In Situ* Top-Down Identification of Intact Proteins Directly from Tissue

Oliver J. Hale and Helen J. Cooper*

Cite This: https://dx.doi.org/10.1021/jasms.0c00226

Read Online

ACCESS | Metrics & More | Article Recommendations | Supporting Information

ABSTRACT: Mass spectrometry imaging (MSI) provides information on the spatial distribution of molecules within a biological substrate without the requirement for labeling. Its broad specificity, i.e., the capability to spatially profile any analyte ion detected, constitutes a major advantage over other imaging techniques. A separate branch of mass spectrometry, native mass spectrometry, provides information relating to protein structure through retention of solution-phase interactions in the gas phase. Integration of MSI and native mass spectrometry ("native MSI") affords opportunities for simultaneous acquisition of spatial and structural information on proteins directly from their physiological environment. Here, we demonstrate significant improvements in native MSI and associated protein identification of intact proteins and protein assemblies in thin sections of rat kidney by use of liquid extraction surface analysis on a state-of-the-art Orbitrap mass spectrometer optimized for intact protein analysis. Proteins of up to 47 kDa, including a trimeric protein complex, were imaged and identified.

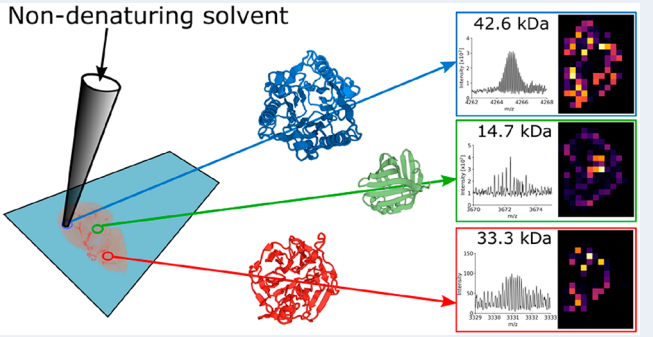

INTRODUCTION

Mass spectrometry imaging (MSI) enables molecules to be spatially mapped throughout a biological substrate, such as a thin tissue section.[1] Typically, MSI is used to map highly abundant, low-mass analytes, e.g., lipids and metabolites. Proteins prove more challenging to image due to their significantly greater mass and lower abundance but nevertheless are a trove of information for the study of disease biology and physiological functions and in the design of therapeutics. A separate but thriving area of mass spectrometry is native MS, so called because proteins are ionized from physiologically mimicking sample conditions in order to retain information on solution structures in the gas phase.[2] Native MS can provide stoichiometric information for protein−protein and protein−ligand complexes through careful optimization of sample conditions, instrument voltages, and gas pressures.[3−6]

Our long-term goal is to combine the benefits of MSI and native MS, i.e., to obtain information on both spatial distribution and tertiary or quaternary structure, through native mass spectrometry imaging (native MSI). Native MSI has thus far only been performed by liquid extraction surface analysis (LESA);[7,8] a schematic for LESA-MSI is shown in Figure 1. LESA entails automated liquid microjunction sampling of the tissue substrate followed by nanoelectrospray ionization (nanoESI). Native LESA has enabled mapping of small proteins (i.e., less than 20 kDa) and abundant intact hemoglobin complexes from vascular features.[7,9] To fully exploit native MSI, an attendant requirement is protein identification, which is achieved by "top-down" fragmentation (MS^n) of intact protein ions within the mass spectrometer to provide amino acid sequence information.[10] This approach is challenging even with purified samples but provides information on single nucleotide polymorphisms and any correlation between post-translational modifications and avoids additional sample preparation required for enzymatic or chemical derivation. Top-down analysis of ions directly from tissue is substantially more difficult due to overlapping signals, salt adducts, and low signal intensity.

Here, we report significant improvements in the detection and identification of intact proteins of higher molecular weights directly from tissue by native LESA-MSI using a detergent-based solvent system and a state-of-the-art Orbitrap mass spectrometer designed for efficient top-down protein analysis. Our results show native LESA-MSI of intact proteins and protein complexes of molecular weight up to 47 kDa analyzed directly from kidney tissue. Proteins were identified

Special Issue: Focus: 2019 Asilomar Meeting - MS Imaging

Received: June 15, 2020
Revised: July 29, 2020
Accepted: July 31, 2020
Published: July 31, 2020

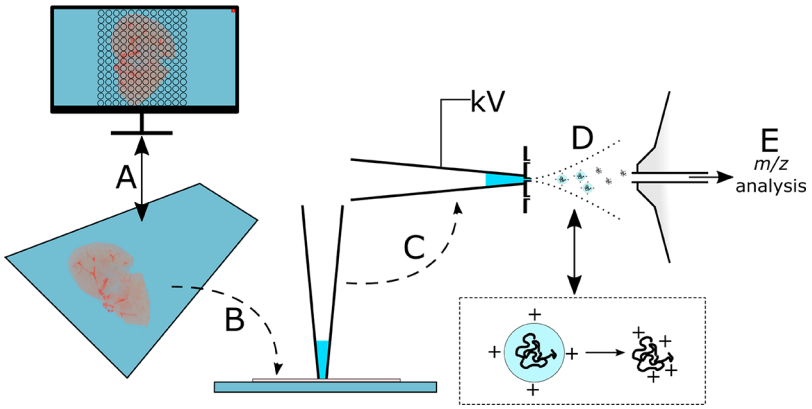

Figure 1. Schematic of the native LESA MSI workflow. (A) A tissue section mounted to a glass slide is scanned into a computer and opened in the image sequence software. A matrix of sampling locations is generated to produce the acquisition sequence. (B) The glass slide is mounted in the LESA robot. (C) A pipet tip is collected by the robot, a volume of extraction solvent is aspirated, and the pipet tip is pressed into contact with the tissue surface. A defined solvent volume is dispensed into the tissue. After a defined period, the solvent is reaspirated and moved to the nanoESI chip. (D) A potential is applied to the pipet tip to initiate electrospray ionization, and multiply charged protein ions are produced. (E) The ions are collected by the mass spectrometer for analysis.

by top-down MS^n, and their spatial distributions were compared to information from existing histological studies.

EXPERIMENTAL SECTION

Materials. Kidney tissue from an orally dosed[11] adult male Hans Wistar rat was the kind gift of Dr. Richard Goodwin (Astra Zeneca). (The drugs were administered as a cassette containing erlotinib, moxifloxacin, olanzapine, and terfenadine (at 10, 25, 10, and 25 mg/kg, respectively).) The animal was euthanized 6 h post dose. All tissue dissection was performed by trained AstraZeneca staff (project license 40/3484, procedure number 10). The kidney was snap frozen and stored at −80 °C until tissue processing.

Tissue was sectioned at −22 °C at 10 μm thickness with a CM1810 Cryostat (Leica Microsystems, Wetzlar, Germany) and thaw mounted to glass microscope slides. Sections were stored at −80 °C until use.

HPLC-grade ammonium acetate was purchased from J. T. Baker (Deventer, The Netherlands), and C8E4 detergent was obtained from Sigma-Aldrich (Gillingham, UK). Nitrogen (>99.995%) and helium (>99.996%) gases used on the mass spectrometer were obtained from BOC (Guildford, UK). MS-grade water was obtained from Fisher Scientific (Loughborough, UK).

LESA. Prior to analysis, the glass slide was mounted to a LESA slide adapter and scanned into LESA Points (version 1.1) at 600 dpi. Sampling locations were defined by overlaying a location array with spacing of 1 × 1 mm. Scans were color-enhanced to improve contrast between the tissue and LESA adapter surface. "Contact" LESA was performed using a Triversa NanoMate (Advion Biosciences, Ithaca, NY) attached to the mass spectrometer. A 5 μL aliquot of extraction solvent (200 mM ammonium acetate + 0.125% C8E4) was aspirated from a solvent reservoir into the conductive pipet tip and moved to the location above the tissue. For imaging analysis, the location spacing was 1 × 1 mm, the minimum allowed by the software (ChipSoft 8.3.3, LESA Points 1.1). (Note that the actual sampled area has a diameter of ∼600 μm, equivalent to the outer diameter of the pipet tip.) The tip was pressed into the tissue surface, and 2.5 μL of solvent was dispensed. After 1 min, 3.5 μL was aspirated, and the tip moved to the nanoESI chip. ESI was initiated with a potential of 1.85 kV and backpressure of 0.15 PSI. Sequential analysis of discrete locations on the tissue in this way enabled production of a mass spectrometry image. The LESA workflow is depicted in Figure 1. The analyzed kidney was scanned again postanalysis to show the sampling locations in Figure 2c.

Mass Spectrometry. Mass spectrometry data were acquired on an Orbitrap Eclipse Tribrid MS (Thermo Fisher, San Jose, CA), equipped with the HMR^n option. High-mass calibration and ion optics tuning in the positive ion mode were performed with FlexMix calibration solution (Thermo Scientific). The instrument was set to "Intact Protein" mode, which uses the ion routing multipole (IRM) to trap ions prior to Orbitrap analysis. The IRM pressure was set to 0.008 Torr ("Standard pressure") with high-purity nitrogen (>99.995%). This pressure may be set up to 0.02 Torr ("High pressure") for more efficient trapping of protein complexes, but this was found to suppress signals for smaller proteins. The ion transfer tube temperature was set to 275 °C. The source-induced dissociation (SID) potential was set to 80 V for imaging experiments and between 80 and 100 V for MS^n. The S-Lens RF was 130% to aid desolvation and transmission of protein ions. Ion detection was performed in the Orbitrap mass analyzer, operating at a resolution of 15 000 (at m/z 200) for imaging experiments and 60 000−500 000 as required for additional experiments (high-resolution full scan spectra, MS^n). The normalized automatic gain control target (AGC) was set to 500%, with a maximum injection time of 200 ms. Two transients (microscans) were averaged per scan. Data from each sampled location (i.e., pixel) was collected for 1 min to produce the mass spectrometry image.

MS^n. Protein ions were selected for MS^n on the basis of their abundance following manual inspection of the mass spectra in the imaging data set. MS^n was performed by sampling serial sections to the section imaged, with reference to the ion images to target the location of highest abundance for the analyte of interest. MS^n of abundant ions (RidA^{10+}, holo-alpha-globin^{5+}) was performed directly from a single sampling location with spectra obtained in less than 5 min. MS^3 of RidA (trimer^{10+} → monomer^{5+} → MS^3 products) was also performed in this way. Exclusively, MS^n of regucalcin^{10+} was performed from a single location with the addition of FAIMS Pro (Thermo Fisher, San Jose, CA), operated with a static

https://dx.doi.org/10.1021/jasms.0c00226
J. Am. Soc. Mass Spectrom. XXXX, XXX, XXX−XXX

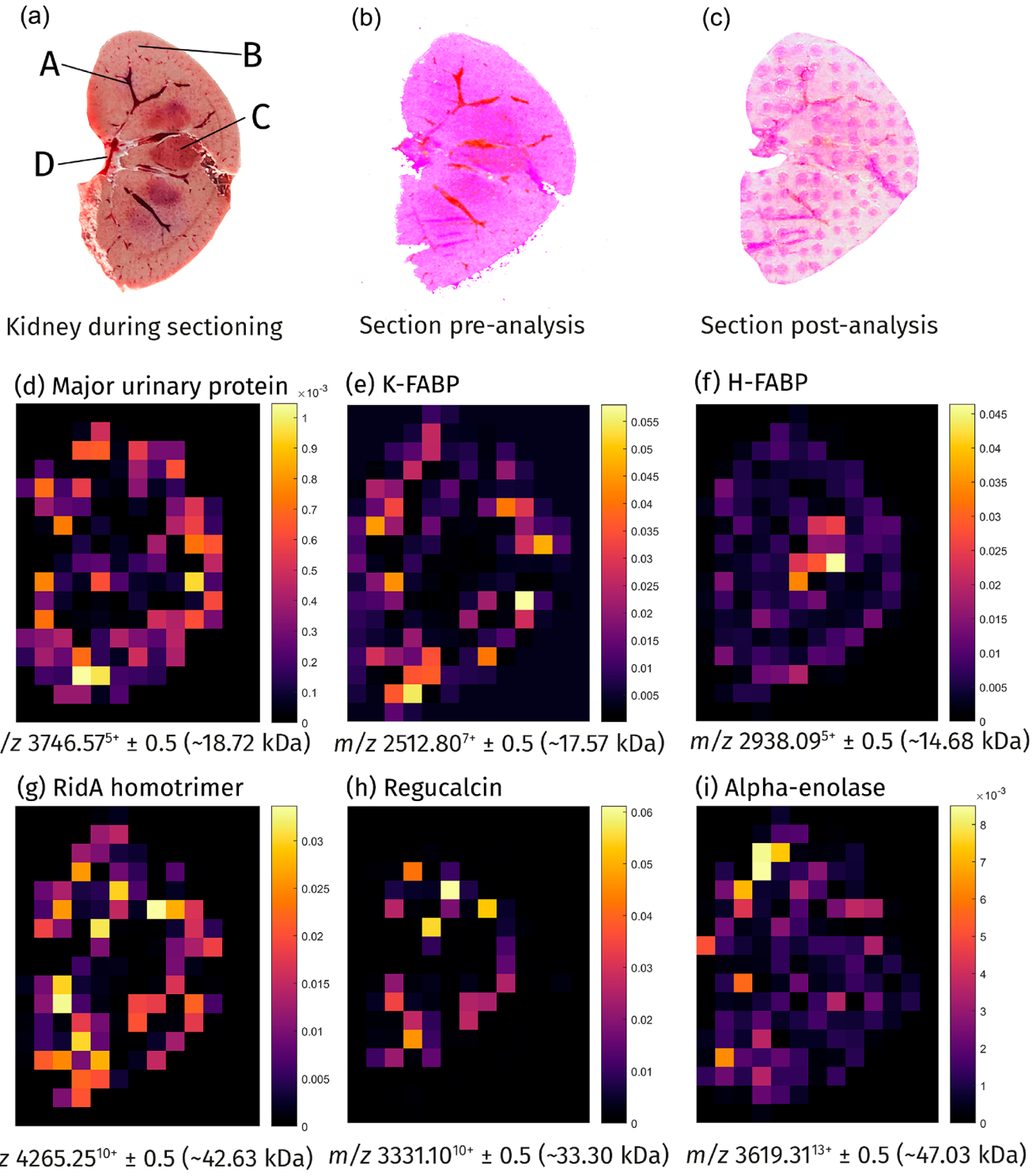

Figure 2. Visualizing intact protein distributions in the rat kidney. (a) Photograph of the kidney with four regions indicated (A, blood vessel; B, cortex; C, medulla; D, renal pelvis). (b) Scan from an optical scanner of the kidney section prior to analysis. (c) Scan of the same kidney section postanalysis with sampling locations visible. Ion images for (d) major urinary protein (MUP), (e) kidney fatty-acid-binding protein (K-FABP), (f) heart FABP, (g) reactive intermediate deiminase A (RidA) homotrimer, (h) regucalcin, and (i) alpha-enolase. Each pixel is 1 × 1 mm. Color bars indicate normalized signal intensity.

compensation voltage (CV) of −31 V, to improve signal-to-noise ratio (S/N) by atmospheric pressure ion mobility separation. Previous work in our laboratory has shown FAIMS to be suitable for transmitting native proteins and improving S/N.[12] Lower-intensity signals (MUP^{7+}, $K\text{-}FABP^{7+}$, H-FABP, and $alpha\text{-}enolase^{13+}$) were analyzed by first pooling five 5 μL LESA extracts followed by direct infusion nanoESI of a 5 μL aliquot using the Triversa NanoMate. MS^n spectra were then acquired for up to 50 min for the lowest intensity protein ion signals. Direct infusion from the pooled aliquot provided more robust ionization and signal than direct sampling for these longer experiments. All MS^n experiments were performed with

https://dx.doi.org/10.1021/jasms.0c00226
J. Am. Soc. Mass Spectrom. XXXX, XXX, XXX−XXX

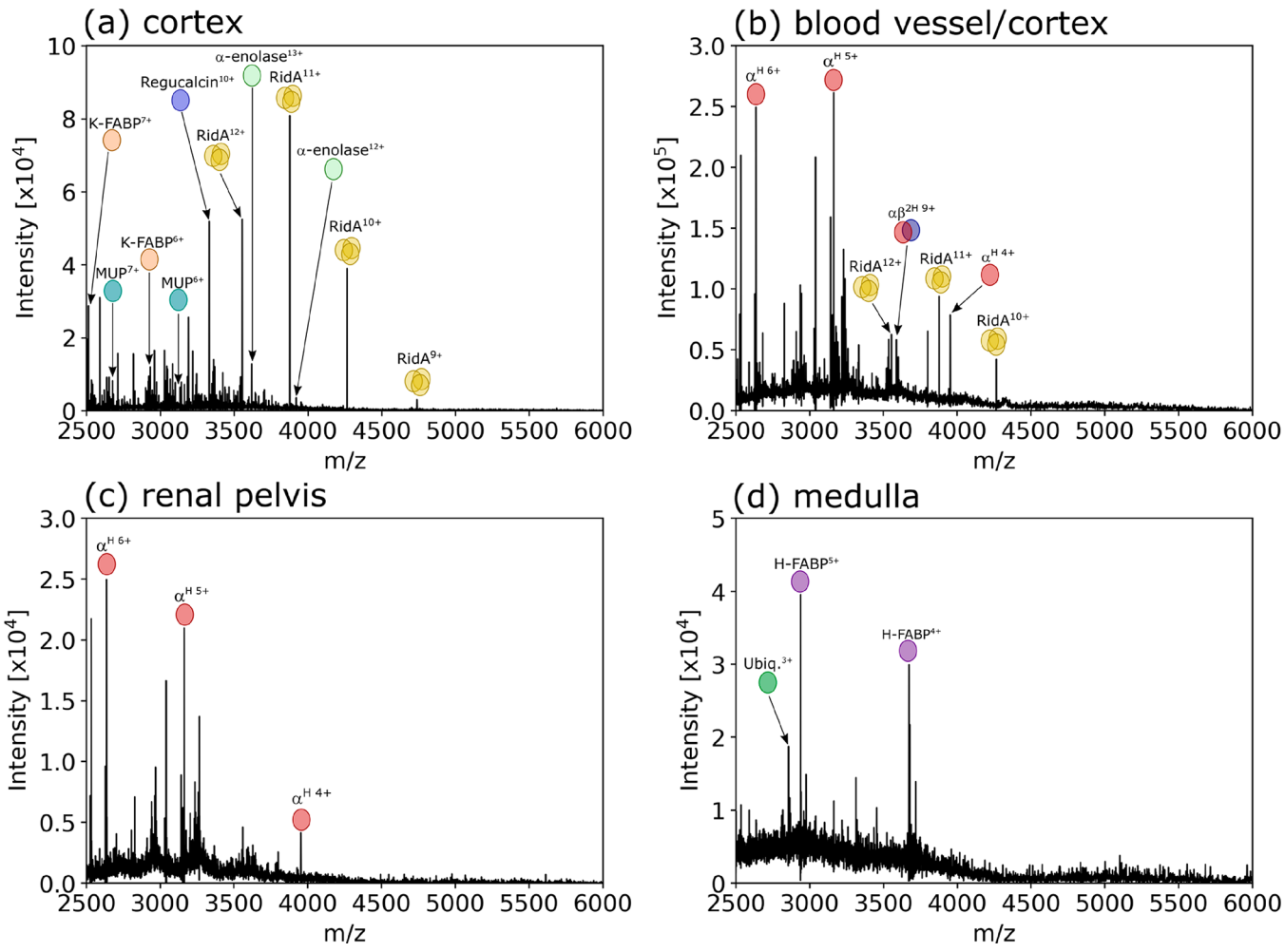

Figure 3. Native LESA mass spectra obtained from locations in four distinct regions of the rat kidney: (a) cortex, (b) a blood vessel within cortex tissue, (c) the renal pelvis, and (d) medulla. The panels correspond to pixels 43, 57, 107, and 111 of the images in Figure 2, respectively. Abbreviations: K-FABP, kidney fatty-acid-binding protein; MUP, major urinary protein; RidA, reactive intermediate deiminase A; α^{H}, holo-alpha-globin; $\alpha\beta^{2H}$, holo-alpha/beta-globin dimer; Ubiq., ubiquitin; H-FABP, heart fatty-acid-binding protein.

ion trap isolation using an isolation window of m/z 1 to 5 depending on the presence of adjacent, unrelated signals to the ion of interest. Based on preliminary studies, the following fragmentation techniques were employed: collision-induced dissociation (CID; MUP, regucalcin, H-FABP) and higher-energy collision dissociation (HCD; K-FABP, RidA, holo-alpha-globin, alpha-enolase).

MS Image Processing. Summed mass spectra for each pixel were generated in FreeStyle (version 1.4, Thermo Scientific) and exported in the Thermo raw format. These files were then converted to mzML by msconvert (Version 3.0, ProteoWizard Software Foundation).[13] The image file was produced with imzML converter (version 1.3).[14] All mzML files were imported and processed with the "pixel per file" option. The resulting imzML file was opened in SpectralAnalysis (version 1.2.1).[15] Top-hat baseline subtraction was applied to each spectrum followed by total ion current (TIC) normalization and zero-filling with the "Orbitrap" option. Individual ion images were produced with a window of $m/z \pm 0.5$.

Protein Identification. Proteins were identified by combining information from low-resolution and high-resolution full scan MS data and top-down MS^n experiments. Low-resolution full scan spectra provided average mass information and were deconvoluted using the Respect algorithm in BioPharmaFinder 3.1 (Thermo Fisher Scientific). High-resolution full scan spectra were deconvoluted using the Xtract algorithm in BioPharmaFinder 3.1, and FreeStyle 1.4. MS^n spectra were manually interrogated to build a zero-charge peak list, which was imported into ProSight 4.1 and searched against the proteome of *Rattus norvegicus* (Uniprot Proteome: UP000002494, downloaded November 2019). The precursor monoisotopic mass tolerance was set to 1 kDa to allow for hits including small bound ligands, the fragment ion tolerance was set to 20 ppm, and the minimum fragment match was set to 1. Tentative identifications were provided by ProSight, with further assignment of MS^n signals performed manually using MS-Product (ProteinProspector, v 5.24.0, http://prospector.ucsf.edu/prospector/mshome.htm, UCSF) to predict fragment m/z.

RESULTS AND DISCUSSION

Figure 2a shows a photograph of the rat kidney during sectioning with four key regions indicated: a blood vessel, the outer region (cortex), the inner region (medulla), and the renal pelvis—the region where the major blood vessels enter and exit the kidney. Examples of ion images for proteins detected with various distributions throughout the kidney are

https://dx.doi.org/10.1021/jasms.0c00226
J. Am. Soc. Mass Spectrom. XXXX, XXX, XXX−XXX

shown in Figure 2d−i. For example, major urinary protein (MUP), K-FABP, and RidA were detected in the cortex, whereas H-FABP was detected in the medulla. Regucalcin was confined to the inner cortex, and α-enolase was most abundant in the top-left of the kidney cortex. With the exception of RidA, none of these proteins have been previously identified in LESA experiments, and none have been mapped by LESA MSI. Examples of native LESA mass spectra for single pixels obtained from analysis of the rat kidney are shown in Figure 3.

Major Urinary Protein (MUP) and Fatty-Acid-Binding Proteins (FABPs). A protein of molecular weight (MW) 18.72 kDa (m/z 3746.57^{5+}, Figure 2d) was predominantly detected within the renal cortex. The protein was identified as major urinary protein (MUP, UniProt P02761) by accurate mass measurement (Δm = −11 ppm) and MS^2 using collision-induced dissociation (CID). (See Figure S1, Supporting Information.) Of 160 potential backbone cleavage sites, 18 were cleaved for a coverage of ∼11%. Cleavage adjacent to certain amino acids, particularly aspartic acid (Asp), is known to occur more readily in native, collision-activated top-down MS^n.[16,17] In this experiment, 67% of the Asp C-terminal bonds were cleaved. (Table S1, Supporting Information, provides sequence and Asp(C-term)-specific sequence coverage for all proteins identified in this article.) MUP is found only in male rats and is a pheromone binder excreted in urine.[18,19] A protein of MW 17.57 kDa (m/z 2512.80^{7+}, Figure 2e) exhibited a similar distribution to MUP. The protein was identified by HCD MS^2 (see Figure S2, Supporting Information) as a chain derived from MUP (residues 29−179, UniProt P02761, Δm = 0.7 ppm). Existing literature refers to this protein as both 15.5 kDa fatty-acid-binding protein (15.5 kDa FABP) and kidney-FABP (K-FABP).[20,21] The former appears to have arisen as a consequence of mass estimation from SDS-PAGE in early work but is clearly erroneous given that its mass has been established as ∼17.6 kDa by more accurate techniques. Throughout this work, we have used the latter to avoid confusion between the name and the molecular weight (although we note that the designation is sometimes applied to keratinocyte FABP).[20,21] Interestingly, MUP is not synthesized in the kidneys; rather, it is absorbed into renal proximal tubules.[22] Once absorbed, MUP may undergo proteolysis,[18] forming K-FABP, which previous immunohistology studies have shown to be detectable throughout the cortex of the kidney.[20] Ion images (see Figure S2a−c, Supporting Information) show the greatest abundance of K-FABP in the cortex and that it is essentially absent in major blood vessels and medulla tissue. A protein unrelated by amino acid sequence but similar in its function of binding fatty acids,[20] heart FABP (H-FABP, UniProt P07483, Δm = −10 ppm, see Figures 2f and S3, Supporting Information), was identified by CID MS^2 and revealed to be differently distributed to MUP and K-FABP, exhibiting the greatest signal intensity in medulla tissue. This observation is in agreement with a previous immunohistology study, which found H-FABP located within the nephron loop in the medulla and not within the cortex.[21]

Analysis of Proteins of MW > 30 kDa. Figure 2g shows the distribution of the noncovalent homotrimeric assembly of reactive intermediate deiminase A (RidA, UniProt P52759, 42.63 kDa, Δm = 12 ppm). The greatest abundance was detected in regions of the cortex (see also Figure S4, Supporting Information). Previous immunohistology studies have suggested that RidA would be found in cortex tissue.[23,24] Reports tend to have focused on analysis of the ∼14.2 kDa subunit, although prior MS analysis was able to detect the intact trimer.[25] Mapping of the intact complex was possible here by native MSI for the first time, with confirmation of its quaternary structure by MS^n. The RidA trimer (m/z 4265^{10+}) was subjected to HCD MS^2, followed by HCD MS^3 of the 5+ monomer product ion, see Figure S5, Supporting Information. The sequence coverage was ∼4.4%, with 80% of all possible Asp(C-term) cleavages observed.

Figure 2h shows the distribution of a protein of ∼33.31 kDa (also Figure S6a−c, Supporting Information). CID MS^2 of the 10+ ion revealed the protein to be regucalcin (Uniprot Q03336, Δm = 0.5 ppm, sequence coverage = 7.4%, see Figure S6d,e, Supporting Information), a calcium-binding protein found in renal proximal tubule epithelial cells.[26] From the ion image, the distribution is noticeably more limited than for MUP, K-FABP, and RidA, i.e., to the inner cortex, suggestive of greater cell type specificity.

The distribution of the highest molecular weight protein identified here (α-enolase, Uniprot P04764, 47.03 kDa, 15.5 ppm) is shown in Figure 2i. The ion images of each charge state (Figure S7a−c, Supporting Information) are highly comparable, with the most intense signals occurring in cortex tissue in the upper-left of the section. α-enolase is known to be differentially expressed with greater abundance in the kidney cortex, versus the medulla, due to its expression within renal tubular epithelial cells.[27,28] It has been implicated as a prognostic cancer marker, as a target in kidney stone prevention, and as a factor in select autoimmune diseases, making it a potentially interesting target for future native MSI studies.[29−31]

Hemoglobin-Related and Small Proteins. Ion images for intact holo-alpha/beta-globin heterodimer ions ($\alpha\beta^{2H}$, see Figure S8a,b, Supporting Information) and holo-alpha-globin (α^{H}, 15.8 kDa, Figure S8c−e, Supporting Information) show the greatest abundance within blood-vessel-rich regions. HCD MS^2 confirmed the identification of the $\alpha^{H\ 5+}$ ions (See Figure S8f,g, Supporting Information); b and y fragment ions were identified plus a characteristic Δm of ∼616 Da (heme). Hemoglobin heterotetramer signals were not detected; it is possible that the source potential used to improve signals for other protein ions resulted in the dissociation of this delicate complex. Alternatively, a low solution concentration may have led to spontaneous dissociation.[32] In previous native LESA experiments, we have found the Hb tetramer to be scarce, typically limited to large vascular features presumably rich in red blood cells and only detectable with a LESA solvent system comprising ammonium acetate with 5% methanol.[9] The distribution of the 3+ charge state of ubiquitin (m/z 2855.87, 8.56 kDa, Figure S9, Supporting Information) was detected most abundantly within central kidney regions including the medullary tissue, in agreement with previous MALDI-MSI.[33]

CONCLUSIONS

Here, we demonstrate a significant step in the development of native mass spectrometry imaging, enabling the spatial distributions of an intact protein complex (RidA) and monomeric proteins up to 47 kDa to be visualized with consistency across multiple ion charge states. The distributions of MUP, K-FABP, H-FABP, RidA, regucalcin, and α-enolase correlate with existing histological studies, within the limits of current LESA spatial resolution. Challenges remain in terms of throughput and expansion of the range of proteins to those of

https://dx.doi.org/10.1021/jasms.0c00226
J. Am. Soc. Mass Spectrom. XXXX, XXX, XXX−XXX

lower physiological concentration and higher molecular mass. Top-down MS^n of native proteins without additional sample cleanup or concentration was suitable for protein identification. Fragment ion generation by collisional activation was consistent with observations for native protein standard fragmentation (i.e., high propensity for cleavage C-terminal to Asp).[17] Nevertheless, protein identification remains a very manual process that is highly reliant on precursor ion abundance to produce quality fragment ion spectra. Strategies for efficient top-down identification, both instrumentally and in software, are a necessity for future development of native LESA-MSI.

■ ASSOCIATED CONTENT

Supporting Information

The Supporting Information is available free of charge at https://pubs.acs.org/doi/10.1021/jasms.0c00226.

Extended data, including ion images for multiple charge states of each protein, and MS^n spectra (PDF)

■ AUTHOR INFORMATION

Corresponding Author

Helen J. Cooper − *School of Biosciences, University of Birmingham, Edgbaston B15 2TT, U.K.;* orcid.org/0000-0003-4590-9384; Email: h.j.cooper@bham.ac.uk

Author

Oliver J. Hale − *School of Biosciences, University of Birmingham, Edgbaston B15 2TT, U.K.;* orcid.org/0000-0002-2286-5780

Complete contact information is available at: https://pubs.acs.org/10.1021/jasms.0c00226

Notes

The authors declare no competing financial interest.

Supplementary data supporting this research is openly available from the University of Birmingham data archive at DOI: 10.25500/edata.bham.00000523.

■ ACKNOWLEDGMENTS

H.J.C. and O.J.H. are funded by EPSRC (EP/S002979/1). The Orbitrap Eclipse mass spectrometer and FAIMS Pro device used in this work were funded by BBSRC (BB/S019456/1).

■ REFERENCES

(1) Caprioli, R. M.; Farmer, T. B.; Gile, J. Molecular imaging of biological samples: localization of peptides and proteins using MALDI-TOF MS. *Anal. Chem.* **1997**, *69*, 4751−4760.

(2) Leney, A. C.; Heck, A. J. Native Mass Spectrometry: What is in the Name? *J. Am. Soc. Mass Spectrom.* **2017**, *28*, 5−13.

(3) Sharon, M.; Robinson, C. V. The role of mass spectrometry in structure elucidation of dynamic protein complexes. *Annu. Rev. Biochem.* **2007**, *76*, 167−193.

(4) Snijder, J.; Rose, R. J.; Veesler, D.; Johnson, J. E.; Heck, A. J. Studying 18 MDa virus assemblies with native mass spectrometry. *Angew. Chem., Int. Ed.* **2013**, *52*, 4020−4023.

(5) van Duijn, E.; Bakkes, P. J.; Heeren, R. M.; van den Heuvel, R. H.; van Heerikhuizen, H.; van der Vies, S. M.; Heck, A. J. Monitoring macromolecular complexes involved in the chaperonin-assisted protein folding cycle by mass spectrometry. *Nat. Methods* **2005**, *2*, 371−376.

(6) Gault, J.; Donlan, J. A.; Liko, I.; Hopper, J. T.; Gupta, K.; Housden, N. G.; Struwe, W. B.; Marty, M. T.; Mize, T.; Bechara, C.; Zhu, Y.; Wu, B.; Kleanthous, C.; Belov, M.; Damoc, E.; Makarov, A.; Robinson, C. V. High-resolution mass spectrometry of small molecules bound to membrane proteins. *Nat. Methods* **2016**, *13*, 333−336.

(7) Griffiths, R. L.; Sisley, E. K.; Lopez-Clavijo, A. F.; Simmonds, A. L.; Styles, I. B.; Cooper, H. J. Native mass spectrometry imaging of intact proteins and protein complexes in thin tissue sections. *Int. J. Mass Spectrom.* **2019**, *437*, 23−29.

(8) Kertesz, V.; Van Berkel, G. J. Fully automated liquid extraction-based surface sampling and ionization using a chip-based robotic nanoelectrospray platform. *J. Mass Spectrom.* **2010**, *45*, 252−260.

(9) Hale, O. J.; Sisley, E. K.; Griffiths, R. L.; Styles, I. B.; Cooper, H. J. Native LESA TWIMS-MSI: Spatial, Conformational, and Mass Analysis of Proteins and Protein Complexes. *J. Am. Soc. Mass Spectrom.* **2020**, *31*, 873−879.

(10) Chait, B. T. Chemistry. Mass spectrometry: bottom-up or top-down? *Science* **2006**, *314*, 65−66.

(11) Swales, J. G.; Tucker, J. W.; Strittmatter, N.; Nilsson, A.; Cobice, D.; Clench, M. R.; Mackay, C. L.; Andren, P. E.; Takats, Z.; Webborn, P. J.; Goodwin, R. J. Mass spectrometry imaging of cassette-dosed drugs for higher throughput pharmacokinetic and biodistribution analysis. *Anal. Chem.* **2014**, *86*, 8473−8480.

(12) Hale, O. J.; Illes-Toth, E.; Mize, T. H.; Cooper, H. J. High-Field Asymmetric Waveform Ion Mobility Spectrometry and Native Mass Spectrometry: Analysis of Intact Protein Assemblies and Protein Complexes. *Anal. Chem.* **2020**, *92*, 6811.

(13) Chambers, M. C.; Maclean, B.; Burke, R.; Amodei, D.; Ruderman, D. L.; Neumann, S.; Gatto, L.; Fischer, B.; Pratt, B.; Egertson, J.; Hoff, K.; Kessner, D.; Tasman, N.; Shulman, N.; Frewen, B.; Baker, T. A.; Brusniak, M. Y.; Paulse, C.; Creasy, D.; Flashner, L.; Kani, K.; Moulding, C.; Seymour, S. L.; Nuwaysir, L. M.; Lefebvre, B.; Kuhlmann, F.; Roark, J.; Rainer, P.; Detlev, S.; Hemenway, T.; Huhmer, A.; Langridge, J.; Connolly, B.; Chadick, T.; Holly, K.; Eckels, J.; Deutsch, E. W.; Moritz, R. L.; Katz, J. E.; Agus, D. B.; MacCoss, M.; Tabb, D. L.; Mallick, P. A cross-platform toolkit for mass spectrometry and proteomics. *Nat. Biotechnol.* **2012**, *30*, 918−920.

(14) Race, A. M.; Styles, I. B.; Bunch, J. Inclusive sharing of mass spectrometry imaging data requires a converter for all. *J. Proteomics* **2012**, *75*, 5111−5112.

(15) Race, A. M.; Palmer, A. D.; Dexter, A.; Steven, R. T.; Styles, I. B.; Bunch, J. SpectralAnalysis: Software for the Masses. *Anal. Chem.* **2016**, *88*, 9451−9458.

(16) Chen, J.; Shiyanov, P.; Zhang, L.; Schlager, J. J.; Green-Church, K. B. Top-down characterization of a native highly intralinked protein: concurrent cleavages of disulfide and protein backbone bonds. *Anal. Chem.* **2010**, *82*, 6079−6089.

(17) Haverland, N. A.; Skinner, O. S.; Fellers, R. T.; Tariq, A. A.; Early, B. P.; LeDuc, R. D.; Fornelli, L.; Compton, P. D.; Kelleher, N. L. Defining Gas-Phase Fragmentation Propensities of Intact Proteins During Native Top-Down Mass Spectrometry. *J. Am. Soc. Mass Spectrom.* **2017**, *28*, 1203−1215.

(18) Kimura, H.; Odani, S.; Suzuki, J.-i.; Arakawa, M.; Ono, T. Kidney fatty acid-binding protein: Identification as α2U-globulin. *FEBS Lett.* **1989**, *246*, 101−104.

(19) Bocskei, Z.; Groom, C. R.; Flower, D. R.; Wright, C. E.; Phillips, S. E.; Cavaggioni, A.; Findlay, J. B.; North, A. C. Pheromone binding to two rodent urinary proteins revealed by X-ray crystallography. *Nature* **1992**, *360*, 186−188.

(20) Lam, K. T.; Borkan, S.; Claffey, K. P.; Schwartz, J. H.; Chobanian, A. V.; Brecher, P. Properties and differential regulation of two fatty acid binding proteins in the rat kidney. *J. Biol. Chem.* **1988**, *263*, 15762−15768.

(21) Kimura, H.; Odani, S.; Nishi, S.; Sato, H.; Arakawa, M.; Ono, T. Primary structure and cellular distribution of two fatty acid-binding proteins in adult rat kidneys. *J. Biol. Chem.* **1991**, *266*, 5963−5972.

(22) Gomez-Baena, G.; Armstrong, S. D.; Phelan, M. M.; Hurst, J. L.; Beynon, R. J. The major urinary protein system in the rat. *Biochem. Soc. Trans.* **2014**, *42*, 886−892.

(23) Oka, T.; Tsuji, H.; Noda, C.; Sakai, K.; Hong, Y. M.; Suzuki, I.; Munoz, S.; Natori, Y. Isolation and characterization of a novel perchloric acid-soluble protein inhibiting cell-free protein synthesis. *J. Biol. Chem.* **1995**, *270*, 30060−30067.
(24) Schmiedeknecht, G.; Kerkhoff, C.; Orso, E.; Stohr, J.; Aslanidis, C.; Nagy, G. M.; Knuechel, R.; Schmitz, G. Isolation and characterization of a 14.5-kDa trichloroacetic-acid-soluble translational inhibitor protein from human monocytes that is upregulated upon cellular differentiation. *Eur. J. Biochem.* **1996**, *242*, 339−351.
(25) Griffiths, R. L.; Konijnenberg, A.; Viner, R.; Cooper, H. J. Direct Mass Spectrometry Analysis of Protein Complexes and Intact Proteins up to < 70 kDa from Tissue. *Anal. Chem.* **2019**, *91*, 6962−6966.
(26) Fujita, T.; Shirasawa, T.; Uchida, K.; Maruyama, N. Isolation of cDNA clone encoding rat senescence marker protein-30 (SMP30) and its tissue distribution. *Biochim. Biophys. Acta, Gene Struct. Expression* **1992**, *1132*, 297−305.
(27) Arthur, J. M.; Thongboonkerd, V.; Scherzer, J. A.; Cai, J.; Pierce, W. M.; Klein, J. B. Differential expression of proteins in renal cortex and medulla: a proteomic approach. *Kidney Int.* **2002**, *62*, 1314−1321.
(28) Fong-Ngern, K.; Peerapen, P.; Sinchaikul, S.; Chen, S. T.; Thongboonkerd, V. Large-scale identification of calcium oxalate monohydrate crystal-binding proteins on apical membrane of distal renal tubular epithelial cells. *J. Proteome Res.* **2011**, *10*, 4463−4477.
(29) White-Al Habeeb, N. M.; Di Meo, A.; Scorilas, A.; Rotondo, F.; Masui, O.; Seivwright, A.; Gabril, M.; Girgis, A. H.; Jewett, M. A.; Yousef, G. M. Alpha-enolase is a potential prognostic marker in clear cell renal cell carcinoma. *Clin. Exp. Metastasis* **2015**, *32*, 531−541.
(30) Song, Y.; Luo, Q.; Long, H.; Hu, Z.; Que, T.; Zhang, X.; Li, Z.; Wang, G.; Yi, L.; Liu, Z.; Fang, W.; Qi, S. Alpha-enolase as a potential cancer prognostic marker promotes cell growth, migration, and invasion in glioma. *Mol. Cancer* **2014**, *13*, 65.
(31) Fong-Ngern, K.; Thongboonkerd, V. Alpha-enolase on apical surface of renal tubular epithelial cells serves as a calcium oxalate crystal receptor. *Sci. Rep.* **2016**, *6*, 36103.
(32) Manning, L. R.; Jenkins, W. T.; Hess, J. R.; Vandegriff, K.; Winslow, R. M.; Manning, J. M. Subunit dissociations in natural and recombinant hemoglobins. *Protein Sci.* **1996**, *5*, 775−781.
(33) Chaurand, P.; Cornett, D. S.; Caprioli, R. M. Molecular imaging of thin mammalian tissue sections by mass spectrometry. *Curr. Opin. Biotechnol.* **2006**, *17*, 431−436.

https://dx.doi.org/10.1021/jasms.0c00226
J. Am. Soc. Mass Spectrom. XXXX, XXX, XXX−XXX